RSC Advances

Cite this: DOI: 10.1039/c0xx00000x

www.rsc.org/xxxxxx

Effect of structural variation on photovoltaic characteristics of phenyl substituted diketopyrrolopyrroles

Jason Lin,[a] Jianhua Liu,[b] Chunki Kim,[c] Arnold B. Tamayo,[d] Christopher M. Proctor,[a] and Thuc-Quyen Nguyen [*a]

Received (in XXX, XXX) Xth XXXXXXXXX 20XX, Accepted Xth XXXXXXXXX 20XX
DOI: 10.1039/b000000x

Supplementary Information

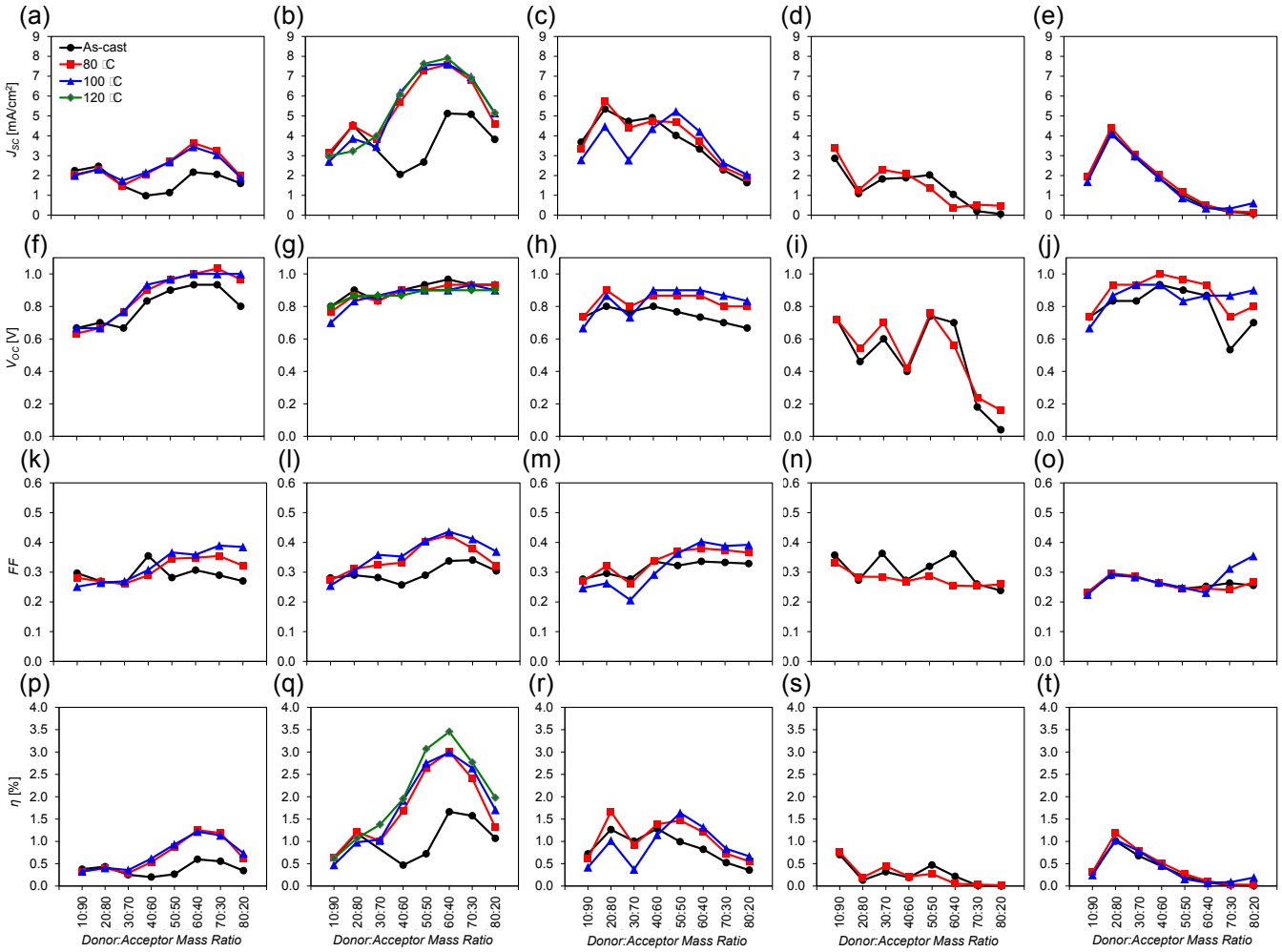

Fig. S1 Solar cell parameters J_{SC} (a-e), V_{OC} (f-j), FF (k-o) and η% (p-t) are plotted as a function of donor:$PC_{71}BM$ mass ratio. DPP donors C6PT1C6 (1st column), C6PT2C6 (2nd column), C6PT3C6 (3rd column), EHPT2C6 (4th column), and C6PT2 (5th column) are shown for as-cast (black circles) films and 10 minute annealed films at 80 ºC (red boxes), 100 ºC (blue triangles), and 120 ºC (green diamonds).

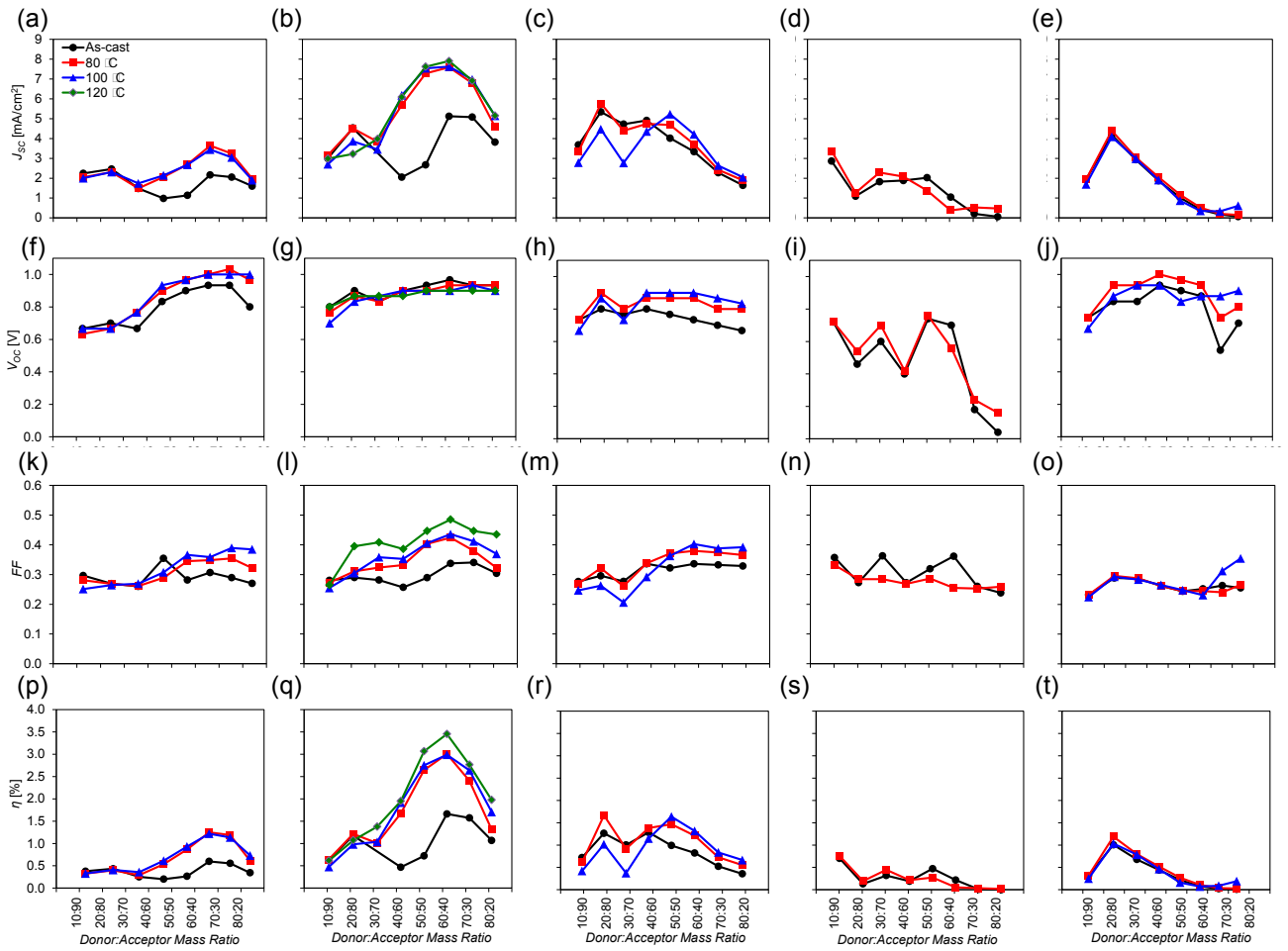

Fig. S2 Solar cell parameters J_{SC} (a-e), V_{OC} (f-j), FF (k-o) and η% (p-t) are plotted as a function of donor:$PC_{71}BM$ molar ratio. DPP donors C6PT1C6 (1st column), C6PT2C6 (2nd column), C6PT3C6 (3rd column), EHPT2C6 (4th column), and C6PT2 (5th column) are shown for as-cast (black circles) films and 10 minute annealed films at 80 ºC (red boxes), 100 ºC (blue triangles), and 120 ºC (green diamonds).

5

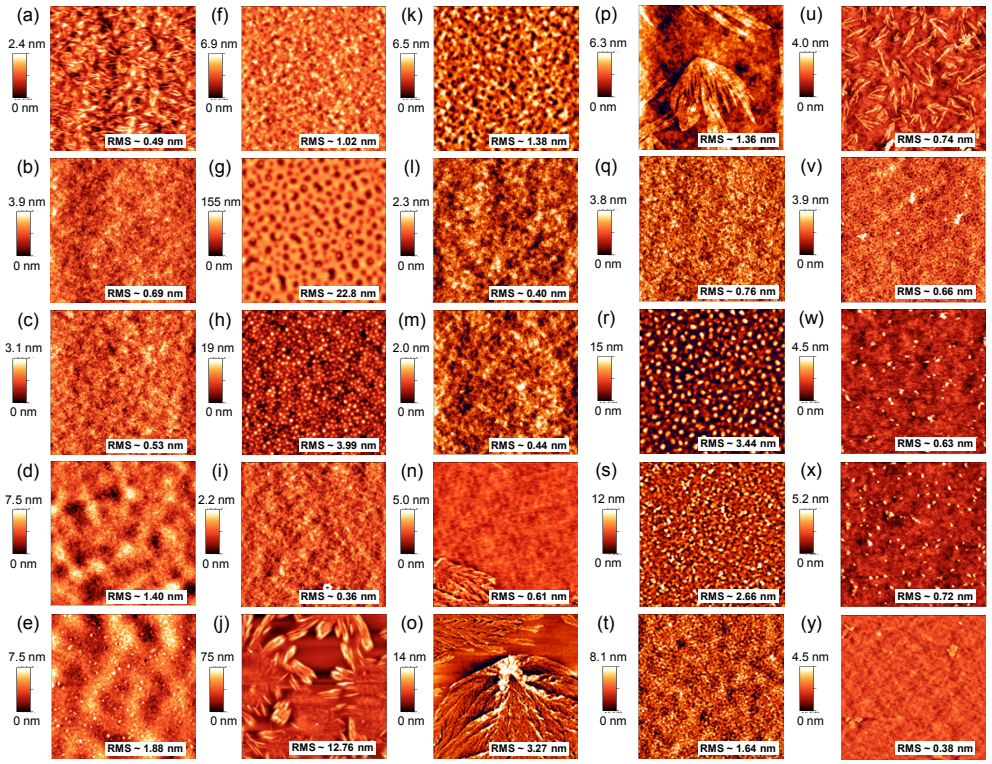

Fig. S3 Topography images for as-cast blend films of C6PT2C6 (a-e), EHPT2C6 (f-j), C6PT2 (k-o), C6PT1C6 (p-t) and C6PT3C6 (u-y) with $PC_{71}BM$ for donor:acceptor blend ratios 10:90 (a, f, k, p, u), 20:80 (b, g, i, q, v), 40:60 (c, h, m, r, w), 60:40 (d, i, n, s, x), and 70:30 (e, j, o, t, y). All image scan sizes are 10 μm × 10 μm.

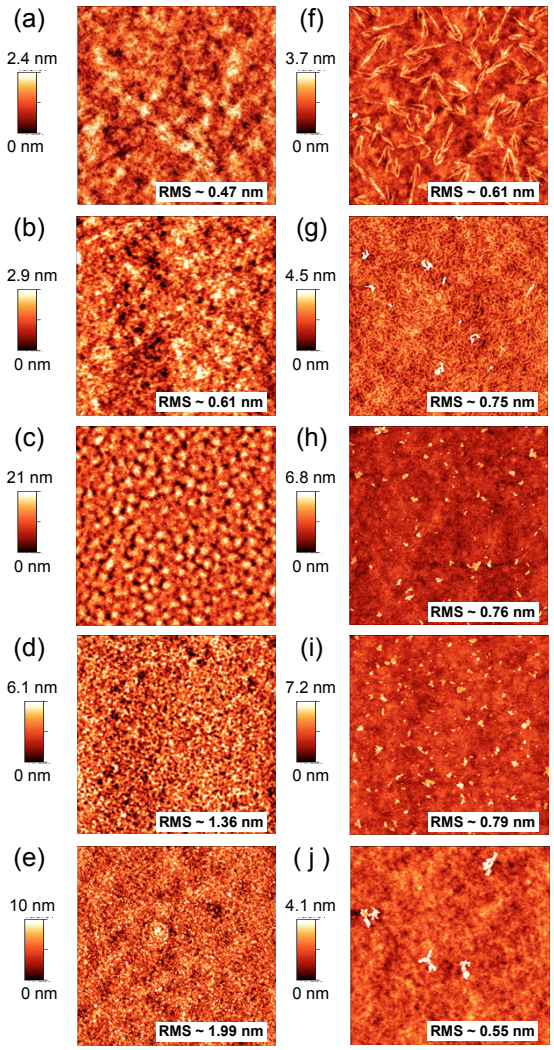

Fig. S4 Topography images for annealed blend films of C6PT1C6 (a-e) and C6PT3C6 (f-j) with $PC_{71}BM$ for donor:acceptor blend ratios 10:90 (a & f), 20:80 (b & g), 40:60 (c & h), 60:40 (d & i), and 70:30 (e & j). Films where annealed at 80 ºC for 10 minutes. All image scan sizes are 10 µm × 10 µm.

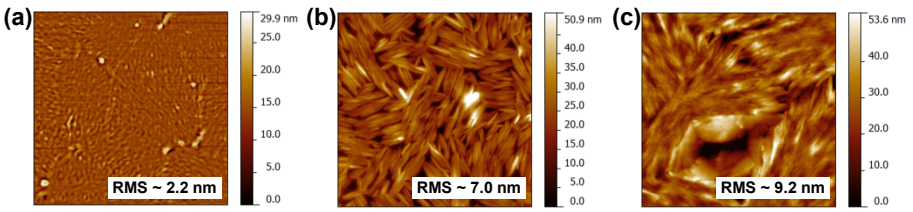

Fig. S5 Topography image of a newly prepared pristine EHPT2C6 film (a) and the same film after 24 hours (b). Also shown is the topography for the 80:20 EHPT2C6:$PC_{71}BM$ films (c). All image scan sizes are 10 µm × 10 µm.

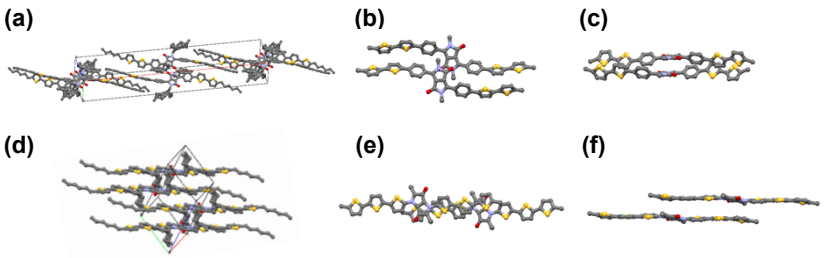

Fig. S6 Single crystal molecular packing for EHPT2C6 ((a)−(c); a unit cell viewed from side (a), b axis (b), and c axis (c)) and SMEHDPP ((d)−(f); a unit cell viewed from side (d), c axis (e), and a axis (f))

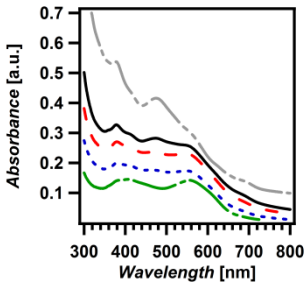

Fig. S7 As-cast absorptions of C6PT3C6 with donor:$PC_{71}BM$ blend ratios of 0:100 (double dotted dashed grey line), 20:80 (solid black line), 40:60 (dashed red line), 60:40 (dotted blue line), and 80:20 (dotted-dashed green line).

Relationship between annealing and electron mobility

Table 2 shows that the optimized C6PT2C6:$PC_{71}BM$ device yields an electron mobility which is nearly two orders of magnitude greater than the optimized C6PT2C6:$PC_{71}BM$ device. To investigate this result we measured the electron mobility of the optimized devices as a function of annealing temperature (Fig. S8). Figure S8 shows that the blend film electron mobility for the optimized C6PT1C6:$PC_{71}BM$ and C6PT2C6:$PC_{71}BM$ devices increases from 10^{-4} to 10^{-6} cm^2/Vs when going from as cast to 120 ^0C annealing. This result shows that annealing significantly enhances the electron mobility. Since C6PT1C6:$PC_{71}BM$ optimizes at 80 ^0C annealing, the electron mobility remains around 10^{-6} cm^2/Vs. However, C6PT2C6:$PC_{71}BM$ optimizes at 120 ^0C which results in an electron mobility of around 10^{-4} cm^2/Vs. The enhanced electron mobility is likely to aid in charge collection from the acceptor phase and may explain why the optimized C6PT2C6:$PC_{71}BM$ device yield a greater short circuit current and fill factor relative to C6PT1C6:$PC_{71}BM$.

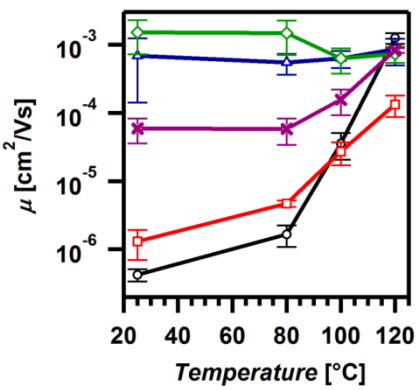

Fig. S8 Electron mobility of optimized blend films of C6PT1C6 (black circles), C6PT2C6 (red squares), C6PT3C6 (blue triangles), EHPT2C6 (green diamond) and C6PT2 (purple ×) as a function of annealing temperature. Films where annealed for 10 minutes at a given temperature.

Relationship between device optimization temperature and exciton harvesting

As discussed earlier, Figure S8 shows that the optimized C6PT2C6:$PC_{71}BM$ device yields a greater electron mobility relative to the optimized C6PT1C6:$PC_{71}BM$ device because it optimized at an elevated annealing temperature where the electron mobility is enhanced. To further probe the driving for device optimization at a specific temperature the blend film photoluminescence was measured as a function of annealing temperature. Figure S9 shows the integrated steady state spectra normalized by the absorption at the excitation

wavelength for the 60:40 C6PT1C6:$PC_{71}BM$ and 60:40 C6PT2C6:$PC_{71}BM$ blend films. The photoluminescence in the 60:40 C6PT1C6:$PC_{71}BM$ blend film is shown to dramatically increase upon annealing at subsequent higher temperatures. In contrast, the 60:40 C6PT2C6:$PC_{71}BM$ blend film only slightly increases upon annealing. An increase in photoluminescence indicates a weaker quenching efficiency of excitons and exciton harvesting. This result show that exciton harvesting significantly drops when C6PT1C6:$PC_{71}BM$ blend films are annealed at elevated temperatures. This result suggests that the C6PT1C6:$PC_{71}BM$ blend films optimize at a lower annealing temperature in order to prevent exciton harvesting losses which would arise at higher annealing temperatures. In comparison, C6PT2C6:$PC_{71}BM$ blend films to not exhibit a significant loss in exciton harvesting upon annealing which may explain why it is able to optimize at an elevated annealing temperature.

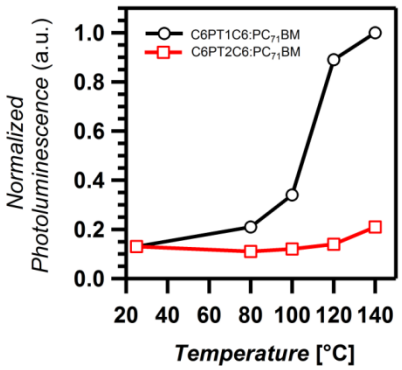

Fig. S9 Photoluminescence as a function of annealing temperature for 60:40 C6PT1C6:$PC_{71}BM$ (black circles) and 60:40 C6PT2C6:$PC_{71}BM$ (red squares) blend films. Integrated photoluminescence was normalized by the absorption of the of each blend film at the 457 nm excitation wavelength.

Relationship between conjugation length and molecular ordering

Relative to C6PT1C6:$PC_{71}BM$ blend films, C6PT1C6:$PC_{71}BM$ blend films exhibit a significant increase in photoluminescence upon annealing at elevated temperatures (Fig S9). It is possible that the molecular ordering is greater in C6PT1C6:$PC_{71}BM$ blend films which induce phase segregation thereby reducing exciton harvesting and increasing photoluminescence. To further investigate the relationship between annealing temperature and molecular ordering, the thin film X-Ray diffraction (XRD) was measured for C6PT1C6:$PC_{71}BM$ and C6PT2C6:$PC_{71}BM$ blend films as a function of annealing temperatures (Fig. S10). Figure S10 shows that the C6PT2C6:$PC_{71}BM$ blend films XRD intensities do not significantly increase when as-cast (Fig. S10a) films are annealed to 80 ^{0}C (Fig. S10b). In comparison, C6PT1C6:$PC_{71}BM$ blend films exhibit a significant increase in XRD intensities when as-cast (Fig. S10c) blends are annealed to 80 ^{0}C (Fig. S10d). This result suggests that C6PT1C6 has a greater affinity for molecular ordering than C6PT2C6. In a previous work the atomic force microscopy (AFM) was used to probe the topography of as-cast and 100 ^{0}C annealed pristine C6PT1C6 and C6PT2C6 films.[1] Both materials exhibited plate like structures in thin films. Relative to C6PT2C6, annealing C6PT1C6 films resulted in a significantly greater increase in the size of the plate like structures. These results suggest that C6PT1C6 has a greater affinity for molecular ordering which induces significant phase segregation in blend films when annealed. An increase in order with decreasing conjugation length is similar to the findings of Liu et al.[2] In summary, increasing the conjugation length of C6PT1C6 by two thiophene units to form C6PT2C6 reduces molecular ordering and phase segregation thereby allowing for device optimization at higher annealing temperatures where electron mobility is enhanced and likely contributes to the greater short circuit current and fill factor observed in the optimized C6PT2C6:$PC_{71}BM$ devices.

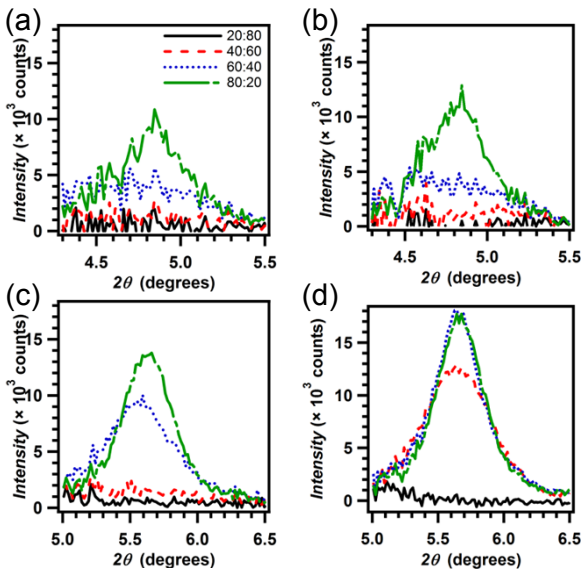

Fig. S10 (a,c) As-cast and (b,d) 80 ºC annealed XRD patterns of C6PT1C6 (a-b) abd C6PT2C6 (c-d) with donor:$PC_{71}BM$ blend ratios of 20:80 (solid black line), 40:60 (dashed red line), 60:40 (dotted blue line), and 80:20 (dotted-dashed green line).

5

References:

1. C. Kim, J. Liu, J. Lin, A. B. Tamayo, B. Walker, G. Wu, and T.-Q. Nguyen, *Chem Mater*, 2012, **24**, 1699–1709.
2. F. Liu, Y. Gu, C. Wang, W. Zhao, D. Chen, A. L. Briseno, and T. P. Russell, *Adv. Mater.*, 2012, **24**, 3947–3951.